Article

Rapid Quantification of Oxidation and UV induced DNA Damage by Repair Assisted Damage Detection-(Rapid RADD)

Noa Gilat, Dmitry Torchinsky, Sapir Margalit, Yael Michaeli, Sigal Avraham, Hila Sharim, Nadav Elkoshi, Carmit Levy, Shahar Zirkin, and Yuval Ebenstein

Rapid Quantification of Oxidation and UV induced DNA Damage by Repair Assisted Damage Detection-(Rapid RADD)

Noa Gilat[1], Dmitry Torchinsky[1], Sapir Margalit[1], Yael Michaeli[1], Sigal Avraham[1], Hila Sharim[1], Nadav Elkoshi[2], Carmit Levy[2], Shahar Zirkin[1] and Yuval Ebenstein[1]**

** Corresponding Authors*

Mailing address:

Noa Gilat - School of Chemistry, Center for Nanoscience and Nanotechnology, Center for Light-Matter Interaction, Raymond and Beverly Sackler Faculty of Exact Sciences, Tel Aviv University, Tel Aviv, Israel

Dmitry Torchinsky- School of Chemistry, Center for Nanoscience and Nanotechnology, Center for Light-Matter Interaction, Raymond and Beverly Sackler Faculty of Exact Sciences, Tel Aviv University, Tel Aviv, Israel

Sapir Margalit- School of Chemistry, Center for Nanoscience and Nanotechnology, Center for Light-Matter Interaction, Raymond and Beverly Sackler Faculty of Exact Sciences, Tel Aviv University, Tel Aviv, Israel

Yael Michaeli- School of Chemistry, Center for Nanoscience and Nanotechnology, Center for Light-Matter Interaction, Raymond and Beverly Sackler Faculty of Exact Sciences, Tel Aviv University, Tel Aviv, Israel

Sigal Avraham- School of Chemistry, Center for Nanoscience and Nanotechnology, Center for Light-Matter Interaction, Raymond and Beverly Sackler Faculty of Exact Sciences, Tel Aviv University, Tel Aviv, Israel

Hila Sharim- School of Chemistry, Center for Nanoscience and Nanotechnology, Center for Light-Matter Interaction, Raymond and Beverly Sackler Faculty of Exact Sciences, Tel Aviv University, Tel Aviv, Israel

Nadav Elkoshi- Department of Human Genetics and Biochemistry, Sackler Faculty of Medicine, Tel Aviv University, Tel Aviv, Israel

Carmit Levy- Department of Human Genetics and Biochemistry, Sackler Faculty of Medicine, Tel Aviv University, Tel Aviv, Israel

* Shahar Zirkin – School of Chemistry, Center for Nanoscience and Nanotechnology, Center for Light-Matter Interaction, Raymond and Beverly Sackler Faculty of Exact Sciences, Tel Aviv University, Tel Aviv, Israel, email: shaharzirkin@gmail.com

* Yuval Ebenstein - School of Chemistry, Center for Nanoscience and Nanotechnology, Center for Light-Matter Interaction, Raymond and Beverly Sackler Faculty of Exact Sciences, Tel Aviv University, Tel Aviv, Israel, email: uv@post.tau.ac.il

Abstract

Knowing the amount and type of DNA damage is of great significance for a broad range of clinical and research applications. However, existing methods either lack in their ability to distinguish between types of DNA damage, or are limited in their sensitivity and reproducibility. The method described herein enables rapid and robust quantification of type-specific single-strand DNA damage. The method is based on Repair-Assisted Damage Detection (RADD) by which fluorescent nucleotides are incorporated into DNA damage sites using type-specific repair enzymes. Up to 90 DNA samples are then deposited on a multi-well glass slide, and analyzed by

a conventional slide scanner for quantification of DNA damage levels. Accurate and sensitive measurements of oxidative or UV-induced DNA damage levels and repair kinetics are presented for both *in-vitro* and *in-vivo* models.

The human body suffers thousands of DNA damage events each day, associated with both endogenous and exogenous damaging factors[1,2]. Normally, DNA damage is rapidly repaired via extensive cellular enzymatic machinery. Failure to repair damaged DNA can result in mutagenesis. This in turn may lead to loss of vital genomic information, genomic instability and the manifestation of diseases such as Parkinson's, Alzheimer's and cancer[3,4].

Reactive oxygen species (ROS) and reactive nitrogen species (RNS), which are produced under oxidative stress during normal metabolic activity or inflammatory response[1,5] are a major cause of endogenous DNA damage. Other triggers for DNA damage are exogenous factors such as exposure to environmental pollutants, chemicals in food and drugs as well as ionizing radiation and solar UV[6,7]. Understanding the type and extent of genomic DNA damage is crucial for both basic research and clinical intervention. The detection and quantification of damage may ultimately be used in determining predisposition to disease, early diagnostics and assessment of response to therapy.

The two main approaches for DNA damage detection rely either on lesion specific antibodies or on the detection of DNA integrity. Antibodies against specific damage lesions are used for colorimetric or fluorescent-based detection of both single and double strand DNA damage markers. Among the methods utilizing this approach are enzyme-linked immunosorbent assays (ELISA), Dot-blot, flow cytometry, and immunohistochemistry[8-12]. The physical integrity of DNA due to single or double strand breaks (SSB & DSB) can be quantified by assays utilizing DNA unwinding such as the comet assay and other electrophoresis based techniques[13-15]. Despite the wide acceptance of these methods, DNA damage detection remains challenging mostly due to lack in sensitivity and poor reproducibility. Moreover, in clinically relevant syndromes, minor changes in the amounts of DNA damage lesions can lead to severe outcomes[16,17]. Addressing such changes

requires high sensitivity and quantitative analysis not easily attained by existing methods. Single molecule DNA analysis may offer an alternative to sensitive quantification of various DNA lesions[18-21]. This approach is based on excising DNA damage lesions enzymatically, followed by *in-vitro* incorporation of fluorescent nucleotides into the gap. Individual DNA molecules are then stretched on a microscope slide for imaging. DNA damage lesions are detected as fluorescent spots along the DNA contour. Despite being highly sensitive, the main limitations of the single molecule approach are its complexity and low throughput which prevent it from being broadly utilized.

Here, we present a robust, high-throughput and highly sensitive assay for the detection and quantification of type-specific single-strand DNA (ssDNA) damage. The assay is based on Repair Assisted Damage Detection (RADD). Specifically, single strand breaks and damage-lesions are replaced with fluorescent nucleotides followed by adsorption of the DNA to a defined compartment on a custom designed multi-well slide. The slide is then imaged by a standard slide scanner, and image analysis is performed to quantify the extent of DNA damage[22]. This new technique, termed Rapid-RADD, enables quantifying a large number of samples in a fast and accurate manner, opening an avenue for large-scale DNA damage and repair screens for research and clinical use.

Materials And Methods

Method overview

Herein is an overview of the entire assay's steps; described in details through the experimental section. **(1)** DNA extraction → **(2)** DNA labeling for oxidation\UV-induced damage with ATTO-550 fluorophore → **(3)** Slide preparation → **(4)** Applying DNA samples onto the activated slide → **(5)** Slide imaging for ATTO-550 fluorophore → **(6)** Total DNA staining with EvaGreen DNA binding dye → **(7)** Slide imaging for EvaGreen DNA binding dye → **(8)** Data Analysis

Cell culture

U2OS (human osteosarcoma) cells were cultured in Dulbecco's modified Eagle's medium (DMEM), supplemented with 10% fetal bovine serum (Gibco), L-glutamine (2 mM) and 1% Penicillin-Streptomycin (10,000 U/mL, Gibco). Cells were incubated at 37 °C with 5% CO_2.

UV irradiation

Cells were washed once with PBS, which was removed from the dish prior to exposure to UVB irradiation (302 nm). Cells were irradiated at doses of 200-1200 J/m^2 in BLX chamber (Vilber). Cell medium was added to the culture prior to DNA extraction.

$KBrO_3$ treatment

Final concentration of 50 mM or 100 mM $KBrO_3$ was added to culture medium for one hour. Cells were washed with PBS twice, and then cell medium was added. DNA was extracted at various time points post $KBrO_3$ treatment.

DNA extraction

For each sample, DNA was extracted from approximately 10^6 cells using the "GenElute-Mammalian Genomic DNA Miniprep Kit" (Sigma) according to manufacturer's instructions.

Mice irradiation and DNA extraction

A total of three C57BL\6JOlaHsd mice at the age of 12-20 weeks were purchased from Harlan Labs. Dorsal hair was shaved two days prior to the experiment, mice were sacrificed and exposed to 10,000 J/m^2 UVB (302 nm). Next, skin samples were flash frozen in liquid nitrogen at the following times points: 5 minutes, 30 minutes, 6 hours and 24 hours. DNA was extracted from thawed samples using the "GenElute-Mammalian Genomic DNA Miniprep Kit" (Sigma) according to manufacturer's instructions.

Labeling oxidation DNA damage

$KBrO_3$-treated DNA samples were labeled for oxidation damage in three consecutive enzymatic reactions. In the first step, each reaction tube contained 500 ng of DNA sample, 1.5 µL of 10x buffer 4 (New England Biolabs, NEB), 1.5 µL of 1 mg/mL bovine serum albumin solution (NEB), 0.3 µL of hOGG1 (ProSpec TechnoGene Ltd.) and ultrapure water to a final volume of 15 µL. The reaction mixture was incubated for 30 minutes at 37 °C. In the second step, 0.5 µL of Endo nuclease IV (10,000 U/mL, NEB) was added to the reaction, and it was incubated for additional 30 minutes at 37 °C. In the final step, the following were added into each reaction tube: 1.5 µL of 10x buffer 4 (NEB), 1.5 µL of 1 mg/mL bovine serum albumin solution (NEB), 0.2 µL of 50 mM NAD^+ (NEB), deoxynucleotides (A,G,C (sigma) and fluorescent ATTO-550-UTP (Jena biosciences GMBH)) to a final concentration of 100 nM, 0.4 µL of Bst DNA polymerase, Large fragment (8,000 U/mL, NEB), 0.2 µL of Taq DNA ligase (40,000 U/mL, NEB) and ultrapure water to a final

volume of 30 µL. The reaction mixture was incubated for 30 minutes at 65 °C. The labeled DNA samples were purified from excess fluorophores using "Oligo Clean & Concentrator" columns (Zymo research), according to manufacturer's recommendations, with two washing steps for optimal results.

Labeling UV-induced DNA damage

UV-irradiated DNA samples were labeled for UV damage in three consecutive enzymatic reactions. In the first step, each reaction tube contained 500 ng of DNA sample, 1.5 µL of 10x buffer 4 (NEB), 1.5 µL of 1 mg/mL bovine serum albumin solution (NEB), 0.5 µL of T4 endonuclease V (T4-PDG, 10,000 U/mL, NEB) and ultrapure water to a final volume of 15 µL. The reaction mixture was incubated for 30 minutes at 37 °C. The second and third labeling steps and the purification step are identical to respective steps in the oxidation damage labeling procedure described above.

Slides preparation

Teflon coated microscope slides (Tekdon, customized well formation, 2 mm diameter wells, 90 wells per slide) were immersed in 0.005% poly-L-lysine solution in water (Sigma), in order to positively charge the surface. The immersed slides were incubated for one hour at 37 °C with mild shaking (25 rpm) and then incubated overnight at 4°C. The following day a blocking step was performed; the slides were washed twice with PBST (0.05% Tween 20) solution and twice with PBS (Sigma), and immersed in a 5% w/v bovine serum albumin (Sigma) solution in PBS. The immersed slides were incubated for one hour at 37 °C with mild shaking (25 rpm) and then incubated overnight at 4 °C. In the final step, slides were washed with water and dried under a flow of nitrogen gas. The slides were used immediately upon drying.

Applying DNA samples onto the activated slides

1 µL of labeled-DNA samples were placed in each well. The optimal DNA concentration for attachment is 10-30 ng per well. Three to five replicates of each sample were placed on the slide. Slides were incubated for 14 minutes at 42 °C and then for 24 minutes at 30 °C, in humid conditions to avoid rapid drying of the wells (Thermoshaker, Eppendorf). The slides were then washed with water and dried under a flow of nitrogen gas.

Total DNA staining

Total DNA was stained with EvaGreen DNA binding dye (Biotium). 1 µL of 1.25 µM dye (90% water, 10% DMSO) was added to each well containing the bound DNA. Wells containing only water and no DNA were also stained, in order to obtain the background signal of the EvaGreen dye in the absence of DNA. Slides were incubated for 30 minutes at room temperature in the dark. The slides were then washed with water and dried under a flow of nitrogen gas.

Slide imaging

Slides were imaged using InnoScan1100 slide scanner (Innopsys). A 532 nm green laser was used to image the ATTO-550 fluorophore. A 635 nm red laser was used to image the ATTO-647 fluorophore. A 488 nm blue laser was used to image the EvaGreen stain. The ATTO-550-labeled DNA was imaged before EvaGreen staining to avoid their co-excitation by the green laser.

Data analysis

Images were analyzed using ImageJ 30. The mean fluorescence intensity inside each well in both channels was extracted. The background signal was determined from the control replicates and

subtracted from the ATTO-550 fluorescence signal (DNA damage labels) in each sample well. To account for background noise in the EvaGreen signal (total DNA), a mean fluorescence signal of all wells containing EvaGreen and no DNA was calculated and subtracted from the EvaGreen signal in each sample well. The calculated ATTO-550 signal in each well was divided by the fluorescence intensity calculated in the EvaGreen channel of the same well, in order to normalize the signal to the actual amount of DNA in the well. Next, the average and standard deviation for each sample were calculated over three to five replicates.

Quantification of DNA damage in individual DNA molecules

The detailed conditions and protocol for the single-molecule DNA damage assay are described in the work of Torchinsky *et al*[23]. Briefly, the DNA was extracted from HEK293 cells and subjected to DNA damage labeling using a type specific repair cocktail, similar to the methods described above for either UV-induced or oxidation DNA damage. Following the labeling procedure, the DNA was extended over activated glass slides. The slides were visualized using a fluorescence microscope (TILL photonics GmbH) and analyzed by an in-house software that counts and calculates the amount of DNA damage sites per length of DNA[24].

Results And Discussion

Rapid-RADD takes advantage of the ability of DNA repair enzymes to specifically recognize damage lesions and create a single-strand gap in the DNA at target damage sites. This is followed by the insertion of fluorescently labeled nucleotides by a DNA-polymerase to fill the gap. The result of this reaction is fluorescence intensity, which is proportional to the level of DNA damage, and can be quantified using a commercial slide scanner. The assay workflow is illustrated in **Figure 1**. First, DNA is extracted from the studied cells/tissue of choice. DNA is treated with a cocktail of specific DNA repair enzymes that recognize and excise different DNA damage lesions (in this case, UV or oxidation DNA damage, **Figure 1.A, B**). Next, DNA polymerase and fluorescent nucleotides are introduced, leading to incorporation of fluorescent nucleotides into the gap (**Figure 1.C**). The labeled DNA is deposited onto a partitioned poly-L-lysine-coated glass slide (**Figure 1.D**), which is then imaged by a standard slide scanner or other fluorescence imager (**Figure 1.E**). Finally, automatic image analysis is used to accurately quantify the amount of DNA damage (**Figure 1.F**).

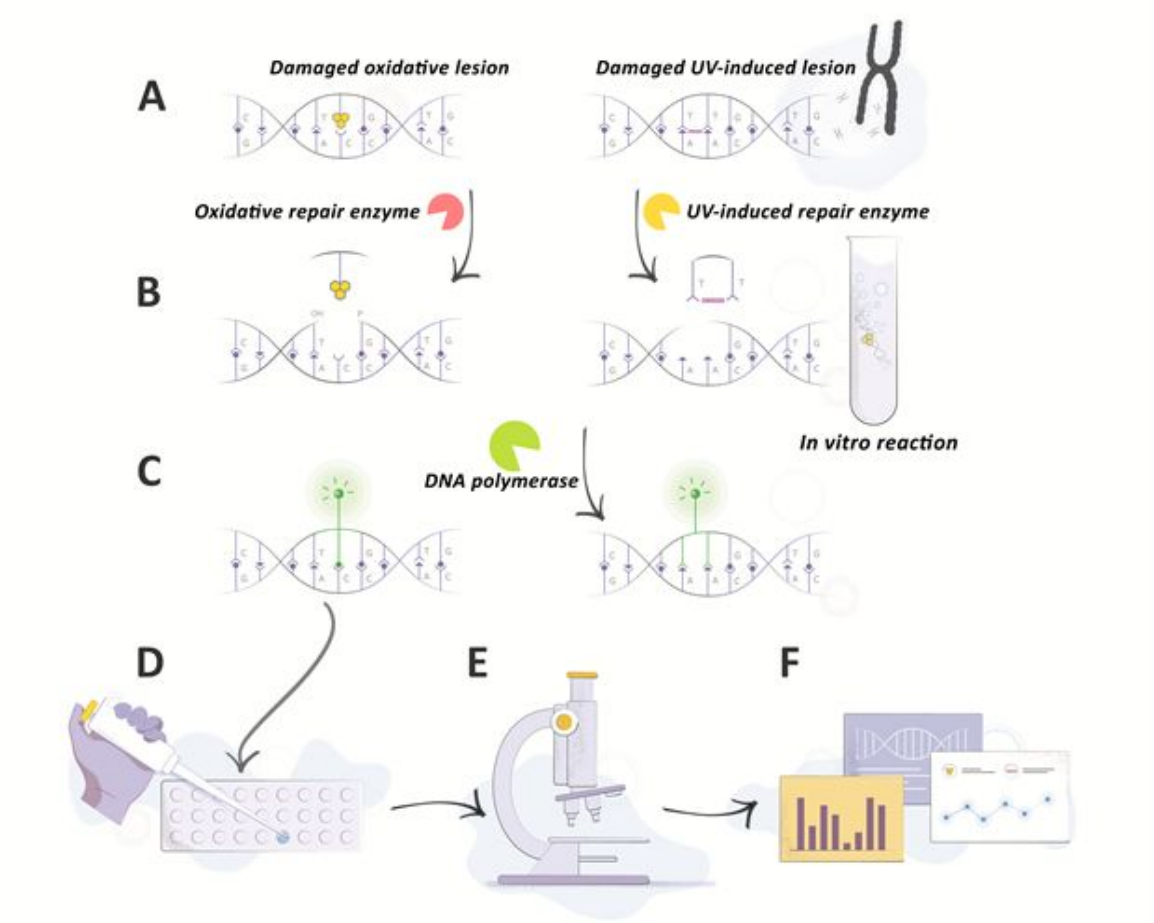

Figure 1. Assay workflow diagram. **(A)** DNA lesions of either UV-induced DNA damage or oxidation DNA damage are recognized by a specific repair enzyme**. (B)** The damaged lesion is excised by the repair enzyme, leaving a gap in the DNA chain. **(C)** DNA polymerase is introduced into the tube, along with fluorescent nucleotides to fill the formed gap. **(D)** The labeled DNA samples are loaded into wells on a positively charged glass slide. **(E)** The slide is imaged on a slide scanner, followed by image analysis **(F)**.

A photograph of an actual multi-well slide loaded with droplets of labeled DNA samples is presented in **Figure 2.A**. This custom-made slide was designed to define 90 wells of 2 mm diameter, each holding 0.5-2.0 µL of sample by surface tension. **Figure 2.B1, B2** display representative slide scanner images, illustrating the increasing UV damage signal (green) and a constant amount of DNA (blue), respectively. U2OS cells were irradiated with increasing levels

of UVB light, and damage levels were assessed as a function of irradiation intensity (302 nm, 200-1200 J/m2). DNA was immediately extracted following irradiation and the T4-PDG repair cocktail was used to excise and label UV-induced lesions with ATTO-550 (Jena bioscience, green). The total DNA was stained using EvaGreen (Biotium, blue). 20 ng of DNA in 1-2 µL volume were loaded onto each well on the multi-well slide. **Figure 2.B1, B2** are images of the same area on the same slide. Each column contains five replicates of the corresponding sample.

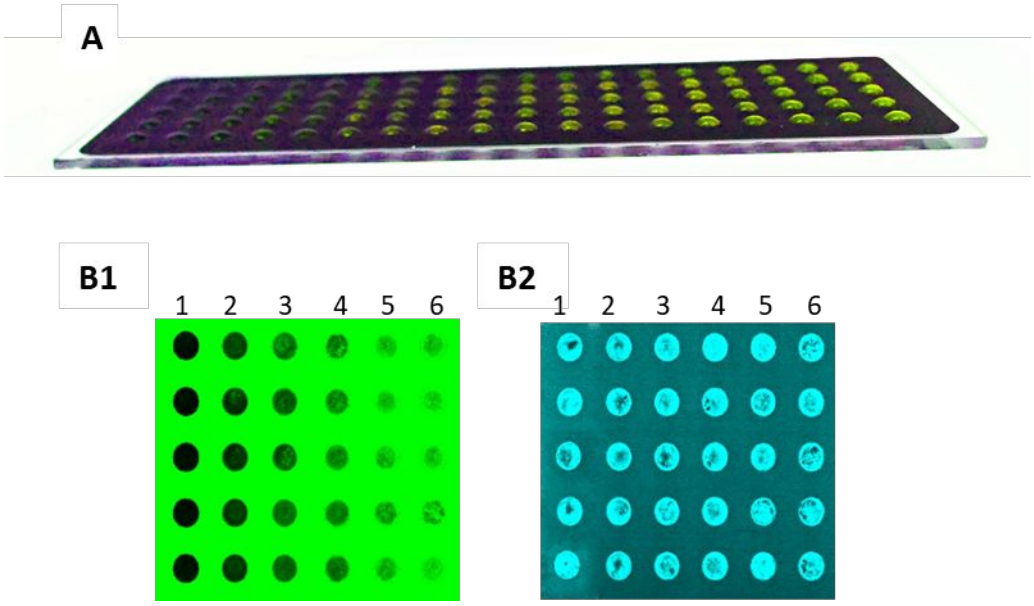

Figure 2. An overview of an experiment in the proposed assay (A) A photograph of the multi-well slide. Teflon coated microscope slide loaded with 1 µL droplets of labeled damaged DNA samples. **(B)** A representative slide scanner image of damaged DNA over the multi-well slide. **(B1)** Increasing levels of the ATTO-550 (green) fluorescence signal corresponding to an increase in UV damage (columns 1-6). (**B2**) The EvaGreen fluorescence signal (blue) is constant and indicates a uniform absorption of the 20 ng DNA to the slide.

In order to optimize the enzymatic repair reactions we first used single molecule detection, an approach extensively used in our lab for sensitive and accurate quantification of DNA damage[19,23]. Labeled DNA molecules are stretched by flow on a microscope slide and damage sites appear as

fluorescent spots along the DNA molecule contour[19]. Despite its complexity, single molecule detection offers direct counting of individual damage sites and is a powerful tool for optimization experiments. HEK293 cells were exposed to UVB irradiation (302 nm, 200 J/m^2) or treated with 50 mM H_2O_2 to induce oxidative stress. Genomic DNA was labeled using a repair cocktail based on T4 endonuclease V (T4-PDG) to target UV-induced lesions or based on the human Oxoguanine Glycosylase 1 (hOGG1) for labeling oxidation damage. DNA samples were stretched and imaged by a sensitive fluorescence microscope and the damage sites were detected and quantified (**Figure 3**).

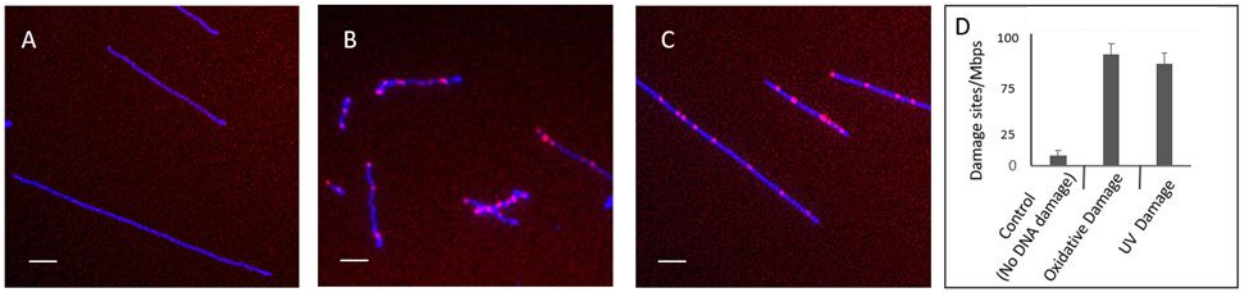

Figure 3. Optimization of labeling reactions by single molecule detection and quantification of DNA damage. HEK293 cells were exposed to DNA damage agents. The DNA samples were labeled using either the T4-PDG repair cocktail (for UVB-irradiated cells) or hOGG1 repair cocktail (for H_2O_2-treated cells), and the damage level was quantified. The DNA was then extracted and the damage sites were labeled with ATTO-647 fluorophores (Jena-Bioscience, red). The DNA molecules were stained with YOYO-1 (Invitrogen, blue) followed by stretching on microscope cover-slip glass slides for imaging and analysis. The damage sites are seen as red dots (ATTO-647 fluorophore) on the blue (YOYO-1) DNA molecules in the representative images in A-C. **(A)** Control cells that were not exposed to any type of DNA damaging agent. **(B)** UVB induced DNA damage (302 nm, 100 J/m2). **(C)** Oxidation induced DNA damage (0.5 hours of treatment with 100 nM H_2O_2). **(D)** A plot bar of the calculated damage sites per Mbp versus the DNA length (in base pairs). Scale bar = 20 μm.

The formation of DNA damage for both UV and H_2O_2 exposures is clearly visualized when comparing to a control sample that was not exposed to any of these damage agents. In order to check the reproducibility of the assay we have conducted a series of eight biological repeat experiments for both H_2O_2 and UV induced DNA damage. We measured a variation of 7% and 9.6% for oxidation and UV damage levels respectively, confirming the robustness of the enzymatic labeling reaction (see Supporting Information, **Figure S1**).

Although single molecule detection provides ultimate sensitivity, it is limited for broad use by the research and clinical communities. Specifically, the assay cannot be used without appropriate expertise and equipment, nor can it deal with a large number of samples simultaneously. In order to lift these limitations we applied the optimized labeling reactions to the partitioned slide platform thus providing a high-throughput, cheap and easy to use assay that can be adapted rapidly to any clinical or research setting.

Rapid-RADD was optimized for quantifying two types of ssDNA damage, namely UV-induced and oxidation DNA damage. Most of the existing assays dealing with UV-induced DNA damage use highly energetic UVC radiation, a portion of the UV spectrum that is almost completely blocked by the atmosphere, and is hence less significant in real-life scenarios. UVB radiation is more relevant to environmental exposures and also generates measurable UV-induced DNA photo-lesions[23] (See Supporting Information, **Figure S2** for comparison between UVB-induced and UVC-induced DNA damage levels). We therefore used this type of radiation for further Rapid-RADD experiments. The second labeling reaction was aimed at detecting oxidation damage, with 8-Oxoguanine being the most common and important damage lesion. In order to address this damage type, we used the hOGG1 based repair cocktail. This reaction efficiently replaces 8-Oxoguanine with a fluorophore for optical detection. To test the assay, we used $KBrO_3$, which is

a strong oxidation agent also known as the food additive Formolene® or E924. The use of $KBrO_3$ in food products is banned in most of the world (but not in the US) as it was shown to induce renal tumors in rats[25] and is classified as a category 2B carcinogen by the International Agency for Research on Cancer (IARC).

U2OS cells were irradiated with increasing levels of UVB light, and damage levels were assessed as a function of irradiation intensity (302 nm, 200-1200 J/m2). DNA was immediately extracted following irradiation, and the T4-PDG repair cocktail was used to excise and label UV-induced lesions. **Figure 4.A** shows a linear dose response for the T4-PDG-labeled samples. Oxidation DNA damage was induced in U2OS cells by exposure to $KBrO_3$ at increasing concentrations for one hour (0, 50 and 100 mM). DNA was extracted from the cells and labeled using the hOGG1 repair cocktail. **Figure 4.B** shows the increase in oxidation DNA damage with exposure to increasing concentrations of $KBrO_3$. These experiments validated the utility of the optimized Rapid-RADD assay for quantifying UV induced and oxidation damage lesions.

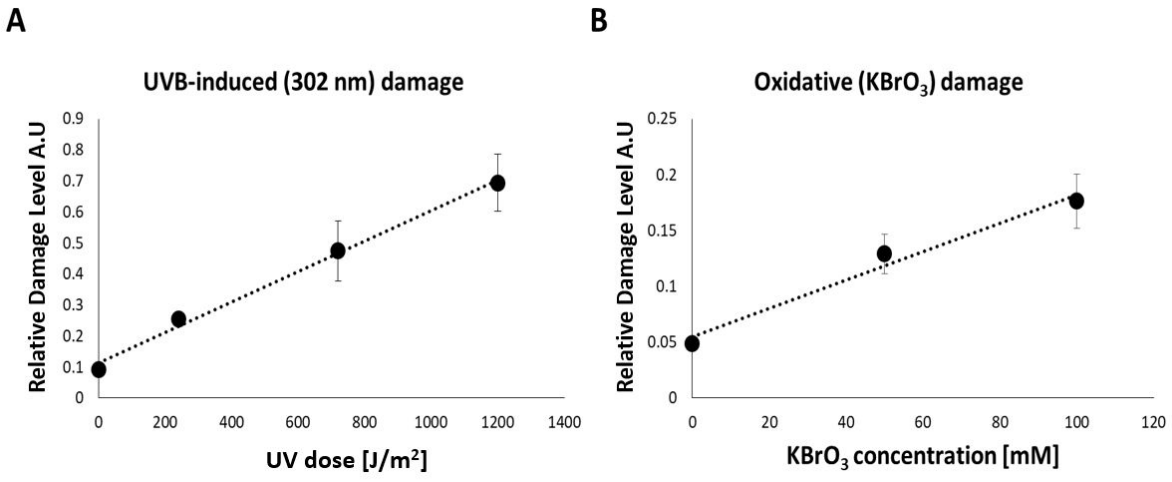

Figure 4. Quantification of oxidation damage and UV-induced damage in U2OS cells. **(A)** Linear increase in damage levels for U2OS cells exposed to increasing doses of UVB light (200-1200 J/m^2) or **(B)** Linear increase in oxidation damage with increasing concentrations of $KBrO_3$ (0-100 mM), followed by DNA extraction. The DNA samples were labeled using either T4-PDG repair cocktail (for UVB-irradiated cells) or hOGG1 repair cocktail (for $KBrO_3$-treated cells), and the damage level was quantified. Data represent mean ± standard deviation (n = 5). All data were collected from two independent experiments.

UVB irradiation also induces oxidative DNA damage *via* creation of ROS that interact with DNA[23]. We have conducted an additional experiment for quantifying the oxidative damage induced in the genomes of UVB irradiated U2OS cells. The extracted DNA was labeled once with the T4-PDG repair cocktail (for direct UV damage), and once with the hOGG1 repair cocktail (for UV induced oxidation damage). The results show an increase in the level of oxidation DNA damage (as well as an increase in the level of UV damage). These results confirm previous observations and are presented as **Figure S3** in the Supporting Information. Finally, the dynamic range of the assay was determined by a controlled spike-in experiment with increasing amounts of a fluorophore-labeled DNA fragment representing a single damage adduct. The limit of detection (LOD) was determined to be 80 damage abducts per 1 mega bp (Mbp) of genomic DNA (see **Figure S4** in the Supporting Information for details). There is no upper limit of detection to the assay, as the sample can always be diluted if the signal of the image reaches saturation. However, under the same scanning conditions required to record the LOD signal of 80 damage adducts/Mbp we also recorded a sample containing the equivalent of 5,000 damage adducts/Mbp (62-fold increase) without saturation (data not shown).

Rapid-RADD is also an attractive tool for assessing the function and efficiency of the cellular DNA repair machinery by probing the levels of damage as a function of time after exposure. We

next set out to measure the repair dynamics of U2OS cells exposed to 50 mM $KBrO_3$ for one hour. DNA was extracted from cells at various time points up to 24 hours post-treatment, allowing native DNA repair to occur. DNA samples from each point were labeled using the hOGG1 repair cocktail and assayed as described above. As expected, the measured damage level immediately after exposure was the highest and it gradually decreased at later time points, indicating repair of the damaged DNA (**Figure 5.A, B**). Notably, although significantly reduced after 24 hours, DNA damage did not return to its basal level as measured in non-treated samples.

As part of the assay development, we aimed to study DNA damage in the context of an *in-vivo* model. DNA damage and repair dynamics in a living organism are extremely challenging to study. However, despite the complexity of these biological processes *in-vivo,* such studies offer more comprehensive information regarding the repair process and its relation to other traits on the organism level, such as nutrition, environmental exposures and disease. We used live mice as a model for quantifying DNA repair *in-vivo*. Three mice were subjected to UVB irradiation, followed by skin DNA extraction at different time points post-irradiation, allowing native DNA repair to occur. As presented in **Figure 5.C**, the highest level of damage was measured immediately after UVB irradiation (5 minutes post-radiation), and the damage level gradually decreased at later time points revealing the dynamic repair profile.

For additional validation, we compared the rapid-RADD results to those obtained with a commercially available cyclobutane pyrimidine dimers (CPD) ELISA kit (Cell Biolabs). DNA samples from four of the irradiated mice were quantified for CPDs with the ELISA kit and showed the expected increase in damage level observed by rapid-RADD. A side-by-side comparison is presented as **Figure S5** in the Supporting Information.

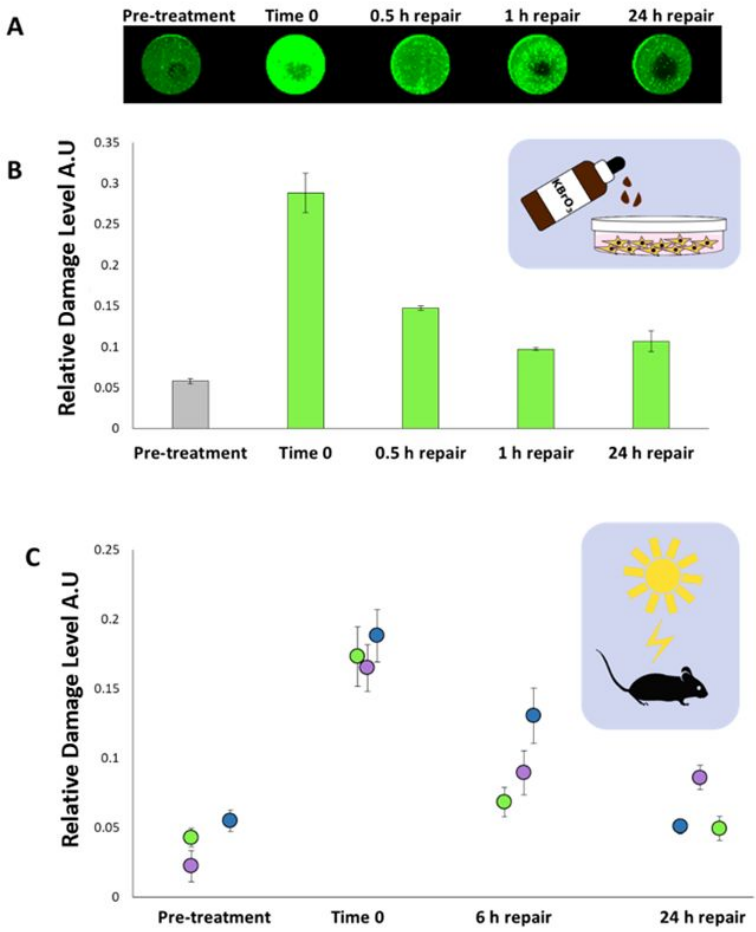

Figure 5. Repair dynamics of oxidation damage and UV-induced damage. **(A)** U2OS cells were incubated with 50 mM $KBrO_3$, then washed and allowed to undergo native DNA damage repair. The DNA was extracted at several time points post-treatment, labeled using the hOGG1 repair cocktail, and further assayed as described above. Representative fluorescence image of wells for each time point (pre-treatment and 0-24 hours post-treatment). **(B)** Quantification results are derived from the slide images and show gradual repair of the damaged DNA, where accurate quantification of the damage level in each sample was calculated. Data represent mean ± standard deviation (n = 5). Each bar represents the averaged results of two independent experiment. **(C)** C57BL\6JOlaHsd mice were irradiated at 10,000 J/m^2 UVB light (302 nm), then allowed to undergo native DNA damage repair. DNA was extracted at several time points post-radiation, then labeled using the T4-PDG repair cocktail, and further assayed as described above. Each differently colored dot represents a different mouse. Data of each dot represents the mean damage level ± standard deviation (n = 5).

In addition to direct quantification of DNA damage levels, the simplicity of the proposed detection concept offers facile multiplexing. By using additional fluorescent colors, the presented labeling reactions may be combined with the quantification of other genomic observables such as epigenetic DNA modifications. As a final proof of concept demonstrating this multiplexing capability, we used a green fluorophore to label UV-induced damage (TAMRA fluorophore) and a red fluorophore to label the 5-hydroxymethylcytosine (5hmC) epigenetic modification (ATTO-647 fluorophore)[19,22,26-28]. Both signals were measured simultaneously for the same DNA sample, potentially allowing the correlation of DNA damage levels with 5hmC content (**Figure S6** in the Supporting Information).

Conclusions

ssDNA damage is the most common form of damage that occurs in DNA, and if not efficiently repaired, might lead to the generation of mutations and the manifestation of diseases, primarily cancer, as well as cell senescence and aging processes[29-32]. In this work, we have presented Rapid-RADD, a simple, high-throughput and highly sensitive method for the quantification of type-specific ssDNA damage. We have shown that ssDNA damage can be fluorescently labeled by specific repair enzymes. For the current slide design, Rapid-RADD enables the quantification of up to 90 samples on a single slide. Our method was found suitable for the detection and quantification of both UV and oxidation-induced ssDNA damage, and was successful in assessing ssDNA damage in conjunction with quantification of the epigenetic modification 5hmC in the same sample. Finally, we were able to characterize and quantify the repair dynamics of DNA damage and specifically, to follow the repair of UV-induced damage *in-vivo*. The developed method is therefore suitable for analyzing a wide variety of DNA samples, and could be easily applied for both clinical and research purposes.

Associated Content

Supporting Information

Additional materials and methods and additional figures

Author Information

[1]School of Chemistry, Center for Nanoscience and Nanotechnology, Center for Light-Matter Interaction, Raymond and Beverly Sackler Faculty of Exact Sciences, Tel Aviv University, Tel Aviv, Israel.

[2]Department of Human Genetics and Biochemistry, Sackler Faculty of Medicine, Tel Aviv University, Tel Aviv, Israel

Author Contributions

YE & SZ designed and supervised the study. YM developed the single-molecule imaging technique. SM developed the multi-well slides used in this study. NG, DT, SA and HS performed the experimental work and data analysis. NE and CL supplied the mice samples which were used in this study. NG, SZ and YE wrote the manuscript. All authors read, commented on, and approved the final manuscript.

Acknowledgments

Y.E. acknowledges support from the BeyondSeq consortium (EC program 634890), the European Research Council Proof of Concept grant (grant no. 767931), the European Research Council starter grant (grant No. 337830), the US National Institute of Health (grant R21ES028015-011), and the Joint Israeli German R&D nanotechnology (grant no. 61976). C.L. acknowledges grant support from the European Research Council (ERC) under the European Union's Horizon 2020 research and innovation programmer (grant agreement no. 726225)

References

1. De Bont, R.; Van Larebeke, N. Mutagenesis 2004, 19, 169-185.
2. Lindahl, T.; Barnes, D. In Cold Spring Harbor symposia on quantitative biology; Cold Spring Harbor Laboratory Press, 2000, pp 127-134.
3. Markesbery, W. R.; Lovell, M. A. Antioxidants & redox signaling 2006, 8, 2039-2045.
4. Tsang, A. H.; Chung, K. K. Biochimica et Biophysica Acta (BBA)-Molecular Basis of Disease 2009, 1792, 643-650.
5. Dedon, P. C.; Tannenbaum, S. R. Archives of biochemistry and biophysics 2004, 423, 12-22.
6. Sinha, R. P.; Häder, D.-P. Photochemical & Photobiological Sciences 2002, 1, 225-236.
7. Wogan, G. N.; Hecht, S. S.; Felton, J. S.; Conney, A. H.; Loeb, L. A. In Seminars in cancer biology; Elsevier, 2004, pp 473-486.
8. Wani, A. A.; Gibson-D'Ambrosio, R. E.; D'Ambrosio, S. M. Photochemistry and photobiology 1984, 40, 465-471.
9. Yoshida, R.; Ogawa, Y.; Kasai, H. Cancer Epidemiology and Prevention Biomarkers 2002, 11, 1076-1081.
10. Manis, J. P.; Morales, J. C.; Xia, Z.; Kutok, J. L.; Alt, F. W.; Carpenter, P. B. Nature immunology 2004, 5, 481.
11. Cosaceanu, D.; Budiu, R.; Carapancea, M.; Castro, J.; Lewensohn, R.; Dricu, A. Oncogene 2007, 26, 2423.
12. Bonner, W. M.; Redon, C. E.; Dickey, J. S.; Nakamura, A. J.; Sedelnikova, O. A.; Solier, S.; Pommier, Y. Nature Reviews Cancer 2008, 8, 957.
13. Singh, N. P.; McCoy, M. T.; Tice, R. R.; Schneider, E. L. Experimental cell research 1988, 175, 184-191.
14. Potter, A. J.; Gollahon, K. A.; Palanca, B. J.; Harbert, M. J.; Choi, Y. M.; Moskovitz, A. H.; Potter, J. D.; Rabinovitch, P. S. Carcinogenesis 2002, 23, 389-401.
15. Gudmundsson, B.; Thormar, H. G.; Sigurdsson, A.; Dankers, W.; Steinarsdottir, M.; Hermanowicz, S.; Sigurdsson, S.; Olafsson, D.; Halldorsdottir, A. M.; Meyn, S. Nucleic acids research 2018, 46, e118-e118.
16. Jackson, S. P.; Bartek, J. Nature 2009, 461, 1071.

17. Richter, C. The international journal of biochemistry & cell biology 1995, 27, 647-653.
18. Lee, J.; Park, H. S.; Lim, S.; Jo, K. Chemical Communications 2013, 49, 4740-4742.
19. Zirkin, S.; Fishman, S.; Sharim, H.; Michaeli, Y.; Don, J.; Ebenstein, Y. Journal of the American Chemical Society 2014, 136, 7771-7776.
20. Lee, J.; Kim, Y.; Lim, S.; Jo, K. Analyst 2016, 141, 847-852.
21. Müller, V.; Dvirnas, A.; Andersson, J.; Singh, V.; KK, S.; Johansson, P.; Ebenstein, Y.; Ambjörnsson, T.; Westerlund, F. Nucleic acids research 2019.
22. Margalit, S.; Avraham, S.; Shahal, T.; Michaeli, Y.; Gilat, N.; Magod, P.; Caspi, M.; Loewenstein, S.; Lahat, G.; Friedmann-Morvinski, D. International journal of cancer 2019.
23. Torchinsky, D.; Michaeli, Y.; Gassman, N. R.; Ebenstein, Y. Chemical Communications 2019, 55, 11414-11417.
24. Jain, N.; Shahal, T.; Gabrieli, T.; Gilat, N.; Torchinsky, D.; Michaeli, Y.; Vogel, V.; Ebenstein, Y. bioRxiv 2019, 587311.
25. Kurokawa, Y.; Maekawa, A.; Takahashi, M.; Hayashi, Y. Environmental health perspectives 1990, 87, 309-335.
26. Shahal, T.; Gilat, N.; Michaeli, Y.; Redy-Keisar, O.; Shabat, D.; Ebenstein, Y. Analytical chemistry 2014, 86, 8231-8237.
27. Nifker, G.; Levy-Sakin, M.; Berkov-Zrihen, Y.; Shahal, T.; Gabrieli, T.; Fridman, M.; Ebenstein, Y. ChemBioChem 2015, 16, 1857-1860.
28. Gilat, N.; Tabachnik, T.; Shwartz, A.; Shahal, T.; Torchinsky, D.; Michaeli, Y.; Nifker, G.; Zirkin, S.; Ebenstein, Y. Clinical epigenetics 2017, 9, 70.
29. Knijnenburg, T. A.; Wang, L.; Zimmermann, M. T.; Chambwe, N.; Gao, G. F.; Cherniack, A. D.; Fan, H.; Shen, H.; Way, G. P.; Greene, C. S. Cell reports 2018, 23, 239-254. e236.
30. Martin, S. A.; Hewish, M.; Sims, D.; Lord, C. J.; Ashworth, A. Cancer research 2011, 71, 1836-1848.
31. Lord, C. J.; Ashworth, A. Nature 2012, 481, 287.
32. Martin, S. A.; McCarthy, A.; Barber, L. J.; Burgess, D. J.; Parry, S.; Lord, C. J.; Ashworth, A. EMBO molecular medicine 2009,` 1, 323-337.

For Table Of Contents Only